Cheiron2007 The 1st AOFSRR Summer School

~ Beamline Practice ~

BL39XU (Magnetic Materials Beamline) 18th September, 2007

Beamline scientists:

Motohiro Suzuki (JASRI/SPring-8, Leader of MCD team)

Naomi Kawamura (JASRI/SPring-8)

Title:

Handling of X-ray polarization and application to X-ray magnetic circular dichroism spectroscopy

Abstract:

To measure X-ray magnetic circular dichroism (XMCD) spectra with high accuracy, a helicity-modulation technique has been developed at BL39XU. Although BL39XU is a hard X-ray beamline with horizontally linear polarization, circularly polarized X-rays are generated by using the diamond X-ray phase retarder (XPR). The helicities are alternated by changing the offset angle of the XPR.

For high-accuracy XMCD measurement, it is necessary to optimize the tuning of the relation among the undulator, monochromator, and XPR precisely; that is, the undulator gap and the XPR condition must be adjusted according to the X-ray energy. On the other hand, the helicity-modulation technique requires a combination of fast switching of the helicity and a phase-sensitive (lock-in) detection system. This technique provides a dichroic signal with less than 0.01% and with a good signal-to-noise ratio. Therefore, extremely high-quality XMCD spectra are obtained in a short acquisition time.

In order to understand polarization control using XPR and the basis of the helicity-modulation method, the following steps are performed in this study.

1. Undulator spectrum measurement by varying the gap value
2. Polarization measurement using a simple polarimeter
3. Synchronous control of undulator gap, monochromator, and XPR
4. X-ray magnetic circular dichroism (XMCD) measurement: comparison of helicity-modulation, helicity-reversal, and magnetic field-reversal methods
5. Element-specific hysteresis measurement using XMCD or fluorescence XMCD measurement (optional)

Optimization of the beamline optics can be achieved by steps 1–3 . From step 4, the effectiveness of the helicity-modulation technique can be established. Step 5 will clarify the advantages of using XPR.

Time Table:

09:00 – 12:00 Controlling the undulator source and beamline optics including X-ray phase retarder
12:00 – 13:00 Lunch
13:00 – 14:50 X-ray magnetic circular dichroism measurement (I)
14:50 – 15:10 Rest
15:10 – 17:00 X-ray magnetic circular dichroism measurement (II)

Beamline:

BL39XU is a hard X-ray beamline covering X-ray energy of 5 – 37 keV.[1,2] Main optical components consist of the undulator, double-crystal monochromator, X-ray phase retarder, and higher-harmonics reduction mirror. Layout of the components of BL39XU is shown in figure 1.

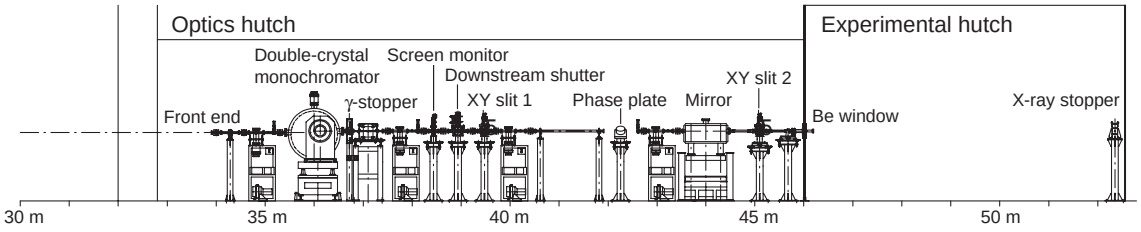

Figure 1. Layout of the optical components of BL39XU.

Undulator:

The light source of BL39XU is an in-vacuum undulator.[3] This undulator provides with extremely high-brilliance X-rays linearly polarized in the horizontal plane. The small X-ray source size and low divergence is perfectly compatible with X-ray diffractive phase retarder [4] for handling the polarization states. Table 1 summarizes the parameters of the undulator.

Table 1. BL39XU undulator source parameters.

Total length /Period /Number of period	4.5 m /32 mm /140
Minimum gap / K_{max}	8 mm /2.46
Tunable energy range (1st, 3rd and 5th)	5 – 70 keV
Peak brilliance	1.4×10^{20} photons/s/mrad^2/mm^2/0.1%b.w./100 mA
Total power /Power density	11 kW (K = 2.3) /470 kW/mrad^2
Polarization	horizontal

Let's measure the undulator spectrum !

The undulator spectrum depends on the gap value (also, the *K* parameter). The energy of the maximum intensity (peak energy) is changeable by changing the gap value. Here, we investigate the relationship between the gap value *G* (mm) and peak energy *E* (keV).

Gap value: *G* (mm)	Peak energy: *E* (keV)
10	
15	
20	
25	
30	
35	
40	
45	
50	

The relation of the peak energy *E* (keV) and the gap value *G* (mm) can be approximated by

$$G = \alpha \ln\left(\frac{\beta}{E} - 1\right) + \gamma, \tag{1}$$

where, α, β and γ are parameters dependent on the undulator property. We determine these parameters by a least-square fitting of our result.

α =

β =

γ =

In SPring-8 users are allowed to change the undulator gap anytime, without giving any influence of the stored electron beam (independent tuning of undulator). At BL39XU the undulator gap is tuned to follow the X-ray energy determined by the monochromator at each energy point while a spectral scan. As a result, very smooth incident X-ray (I_0) spectrum is obtainable as if using a white source. This feature is important to record an EXAFS or XMCD spectrum in a wide energy range.

Put a graph of the undulator spectrum.

Put a graph of the relation between G (mm) and E (keV).

X-ray phase retarder (XPR):

The diamond X-ray phase retarder (XPR) provides us with a freedom of the X-ray polarization: the XPR is used to convert horizontal linear polarization of the source into either circular, vertical, or elliptical polarization.[4] At BL39XU a high rate of circular polarization of $P_C > 0.9$ over 5 – 16 keV is achieved with the use of a synthetic diamond crystal of appropriate thickness.

Let's change the X-ray polarization !

Using the XPR, polarization states is controllable by changing the offset angle $\Delta\theta$ (crystal angle measured from the Bragg condition). The offset angle $\Delta\theta$ for circular ($\pm\pi/2$ retardation) or vertical polarization ($\pm\pi$ retardation) depends on the X-ray energy (wavelength), thickness of the XPR crystal, and reflection plane; the phase retardation δ generated by an XPR is given by [4]

$$\delta = -\frac{\pi}{2}\left[C_{hkl} \cdot \frac{\lambda^3 \sin 2\theta_B}{\Delta\theta} \right] t , \tag{2}$$

where, C_{hkl} represents a constant related to a structure factor of *hkl* Bragg reflection, θ_B and t represent the Bragg angle and the path length of X-rays in the crystal, respectively. When $\delta = \pm\pi/2$ ($\pm\pi$) circularly (vertically) polarized X-rays are generated.

X-ray polarization state can be determined using a simple polarimeter, which consists of Kapton scatter and two scintillation counters as shown in figure 2. When non-polarization component is negligible, the degree of linear polarization is determined by

$$P_L = \frac{I_y - I_x}{I_y + I_x} , \tag{3}$$

where, I_y and I_x represent X-ray intensities scattered vertically and horizontally, respectively. In this case, P_L = 1, 0, and -1 means horizontally linear, circularly, and vertically linear polarization, respectively.

Here, we measure P_L at several X-ray energies using the simple polarimeter. Moreover, we determine the condition of generating circularly and vertically polarized X-rays by analyzing our result.

Thickness of a diamond XPR: t (mm) =		
E (keV)	$\Delta\theta_C$ (arcsec)	$\Delta\theta_V$ (arcsec)
7.0		
7.5		
8.0		
8.5		

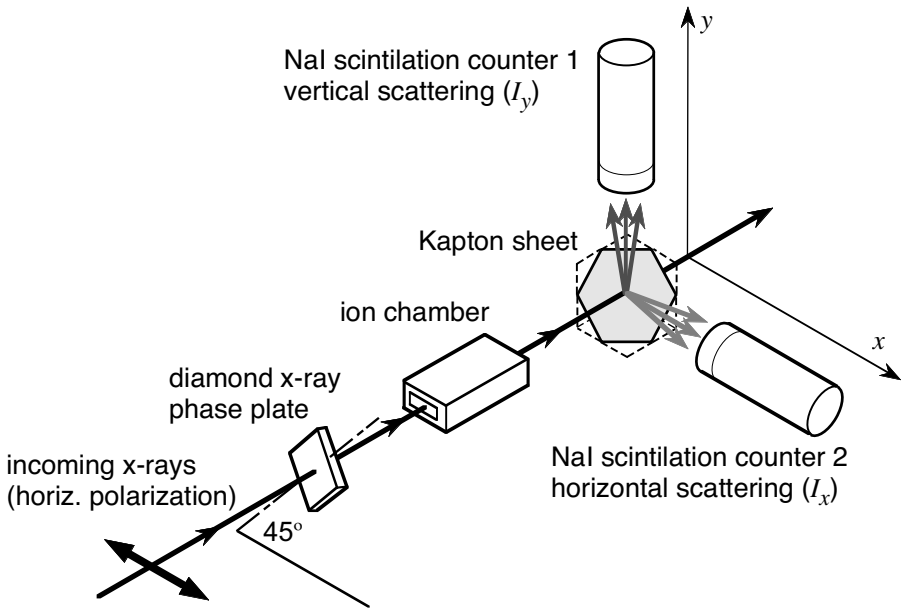

Figure 2. Configuration of the simple polarimeter system.

Put a graph of the result of XPR θ scan.

X-ray magnetic circular dichroism (XMCD):

X-ray magnetic circular dichroism (XMCD) is defined by the difference between the X-ray absorption of a sample for right- and left-circularly polarized X-rays. XMCD is a powerful tool to study the electronic and magnetic states of the ferromagnetic materials.[5,6] In particular, its element-specific feature provides us with detailed information for the magnetic properties.[7]

The XMCD spectrometer consists of a magnet and X-ray detectors. The electromagnet and superconducting magnet are available at BL39XU. In XMCD measurement in the transmission mode, two ionization chambers are used before and after the sample to monitor the incident (I_0) and transmitted (I) X-ray intensities. In the fluorescence mode, an Si drift detector (SDD) is usually used to monitor the fluorescence X-ray intensity from the sample, instead of the I ionization chamber. XMCD spectrum is obtained by measuring and subtracting the X-ray absorption intensities with switching the X-ray helicities at each energy point.

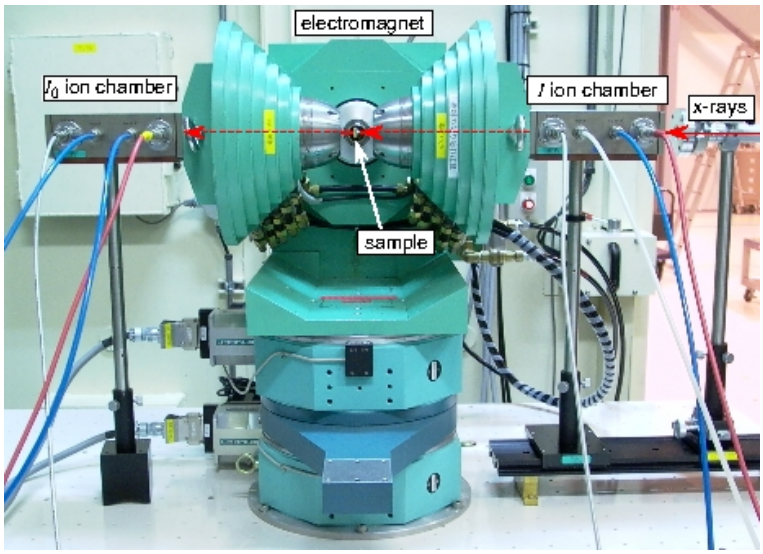

Figure 3. The XMCD spectrometer using the electromagnet.

Let's measure the XMCD spectrum !

Here, we measure an XMCD spectrum in pure Fe foil using a helicity-reversal (static) method. To avoid the demagnetizing effect, magnetic field is applied in-plane of the foil. XMCD spectrum is measured by the transmission-mode using two ionization chambers.

Measurement condition

Applied magnetic field: H (T)=
Sample:
Sample thickness: t (μm) =
Gain of current amplifier: I_0 @ 10 / I_1 @ 10
Energy range: E (keV) = ~
Flipping times / Counting time: / sec

Put a graph of the XMCD spectrum measured by helicity-reversal method.

Helicity-modulation XMCD measurement:

To actualize XMCD measurement with high-accuracy, the helicity-modulation method [8] was developed. This technique allows a measurement of dichroic signals of the order of 0.01% with a good signal-to-noise ratio. Extremely high-quality XMCD spectra are obtainable in a short acquisition time.

The helicity-modulation technique requires a combination of fast switching of the X-ray helicity and a phase-sensitive (lock-in) detection system. Block diagram of the helicity-modulation technique is shown in figure 4.

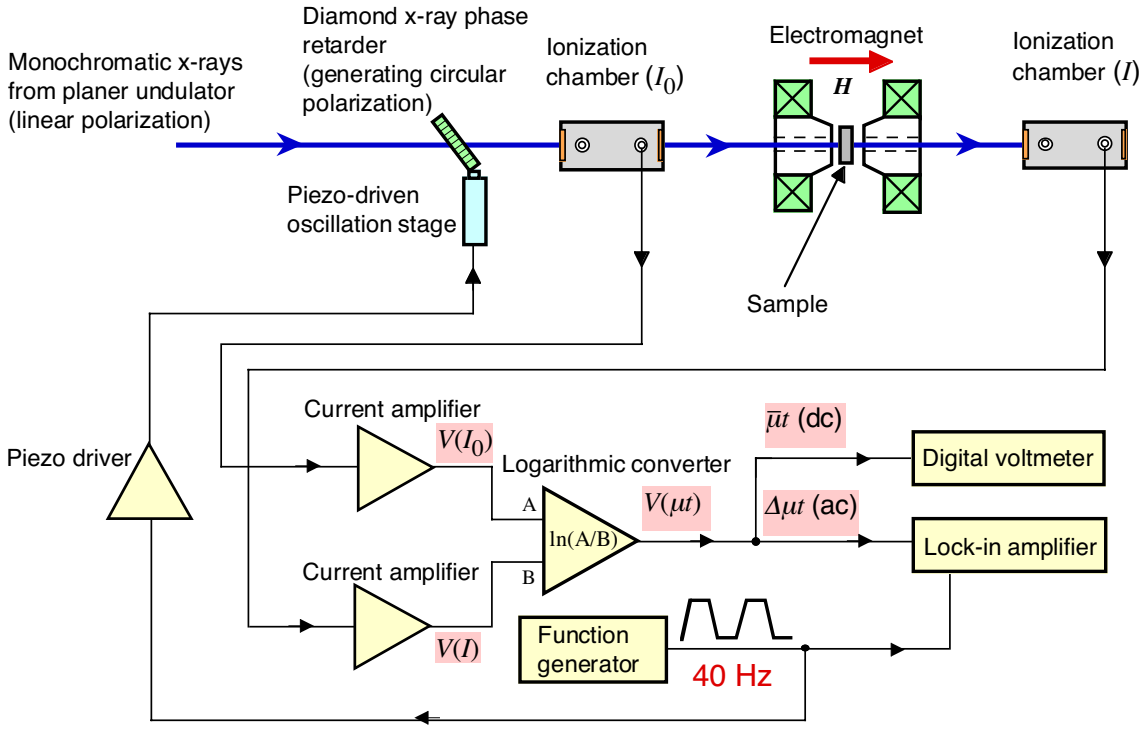

Figure 4. Block diagram of the helicity-modulation technique.

Let's experience the helicity-modulation technique !

Here, we record an XMCD spectrum of the same Fe foil using the helicity-modulation method in the same condition of the helcity-reversal method. Then we compare the obtained spectra using the different methods, with respect to the statistic accuracy, signal-to-noise ratio, amd the acquisition time.

Measurement condition

Applied magnetic field: H (T)=

Sample:

Sample thickness: t (μm) =

Gain of current amplifier: I_0 @ 10 / I_1 @ 10

Energy range: E (keV) = ~

Modulation frequency: f (Hz) =

Accumulation times:

Put a graph of the XMCD spectrum measured by helicity-modulation method.

References:

[1] Show in URL: http://www.spring8.or.jp/en/users/current_user/bl/beamline/BLtable/

[2] H. Maruyama *et al.*: J. Synchrotron Rad. **6** (1999) 1133.

[3] T. Hara *et al.*: J. Synchrotron Rad. **5** (1998) 403.

[4] K. Hirano and H. Maruyama: Jpn. J. Appl. Phys. **36** (1997) L1272.

[5] N. Ishimatsu *et al.*: J. Phys. Soc. Jpn. **76** (2007) 064703.

[6] N. Kawamura *et al.*: J. Phys. Soc. Jpn. **76** (2007) 074716.

[7] A good example is given in : A. Koizumi *et al.*: Phys. Rev. **B61** (2000) R14909.

[8] M. Suzuki *et al.*: Jpn. J. Appl. Phys. **36** (1997) L1272.